Photochemical & Photobiological Sciences

Dynamic Article Links

Cite this: *Photochem. Photobiol. Sci.*, 2011, **10**, 1709

www.rsc.org/pps

PAPER

Ultrafast pump–probe spectroscopy of $IrCl_6^{2-}$ complex in alcohol solutions

Evgeni M. Glebov,*[a,b] Aleksandr V. Kolomeets,[a] Ivan P. Pozdnyakov,[a,b] Victor F. Plyusnin,[a,b] Nikolai V. Tkachenko[c] and Helge Lemmetyinen[c]

Received 10th May 2011, Accepted 13th July 2011
DOI: 10.1039/c1pp05138e

Ultrafast pump-probe spectroscopy (λ_{pump} = 400 nm) was applied to study the primary photophysical processes for the $IrCl_6^{2-}$ complex in methanol and ethanol solutions. The excitation to the LMCT $2U_u'$ state was followed by formation of an intermediate absorption completely decaying with three characteristic times of 300 fs, *ca.* 2.5 ps, and 30 ps. The corresponding processes were interpreted as the $2U_u'^* \rightarrow 1U_g'^*$ electronic transition, vibrational relaxation, and internal conversion to the ground state. Complete recovery of the ground state is consistent with the absence of the photochemical activity of the $IrCl_6^{2-}$ visible LMCT bands.

1. Introduction

The $IrCl_6^{2-}$ complex is stable in aqueous and organic solutions in the absence of free Cl^- ions. Stability and spectral peculiarities make it convenient to study primary photochemical processes both in aqueous[1–8] solutions and in polar organic solvents.[9–15]

The electronic absorption spectrum of $IrCl_6^{2-}$ (curve 1 in Fig. 1) contains strong absorption bands both in the visible and UV regions. $IrCl_6^{2-}$ is a $5d^5$ octahedral complex. The simple assignment of the absorption bands using non-relativistic symmetry (Fig. 2, left side) was performed by Jorgensen.[16,17] Five degenerate d-orbitals of Ir(IV) in octahedral complexes form two equivalent e_g orbitals and three equivalent t_{2g} orbitals. The set of σ-orbitals of six ligands in the crystal field form a_{1g}, e_g and t_{1u} group orbitals, and the set of π-orbitals of ligands form t_{1u}, t_{2u}, t_{1g} and t_{2g} group orbitals. The t_g-sub-shell of the complex has one hole, therefore $d(t_{2g})^5$ configuration of the ground state forms a single doublet term $^2T_{2g}$, which corresponds to the ground state of $IrCl_6^{2-}$. According to ref. 16, the absorption bands in the region of 400–500 nm with an extinction coefficient of *ca.* 4000 M^{-1} cm^{-1} are the bands of ligand-to-metal charge transfer (LMCT). A stronger charge transfer band has a maximum at 232 nm. A relatively weak ($\varepsilon \sim 1000$ M^{-1} cm^{-1}) band at 306 nm belongs to d–d ligand-field transitions.

The photochemistry of $IrCl_6^{2-}$ in water and polar organic solvents is quite different. The mechanisms of the photolysis are wavelength-dependent. The concentration of free chloride anions in solutions is also important. In aqueous solutions, the competition between photoaquation and photoreduction of Ir(IV) to Ir(III) was reported.[2] Excitation in the region of a short-wave charge transfer band (254 nm) leads to the formation of both Ir(IV) and Ir(III) complexes.[2] The $IrCl_5(H_2O)^-$ complex is the photoaquation product, and the $IrCl_5(H_2O)^{2-}$ complex is the photoreduction product. The total quantum yield of 0.03 is independent of the concentration of free Cl^- ions in solution.[2]

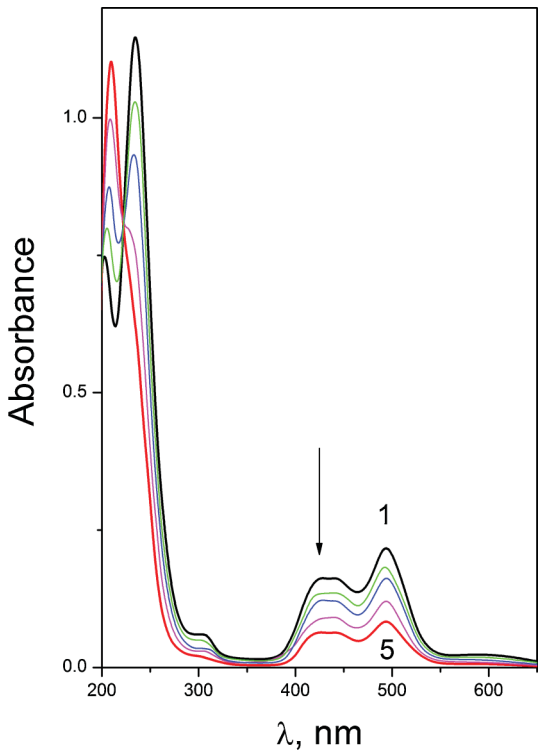

Fig. 1 The change in the UV spectrum of the $IrCl_6^{2-}$ complex in deaerated methanol solution under irradiation at 308 nm (XeCl laser, 17 mJ $pulse^{-1}$). Temperature, 300 K; initial concentration, 5.4×10^{-4} M; cuvette thickness, 0.086 cm; curves 1–5 denote 0, 35, 70, 160, 260 laser pulses.

[a]*Institute of Chemical Kinetics and Combustion, 3 Institutskaya St., 630090, Novosibirsk, Russian Federation. E-mail: glebov@kinetics.nsc.ru; Fax: 7 383 3307350; Tel: 7 383 3332385*
[b]*Novosibirsk State University, 2 Pirogova St., 630090, Novosibirsk, Russian Federation*
[c]*Institute of Materials Chemistry, Tampere University of Technology, P.O. Box 589, 33101, Tampere, Finland. E-mail: nikolai.tkachenko@tut.fi*

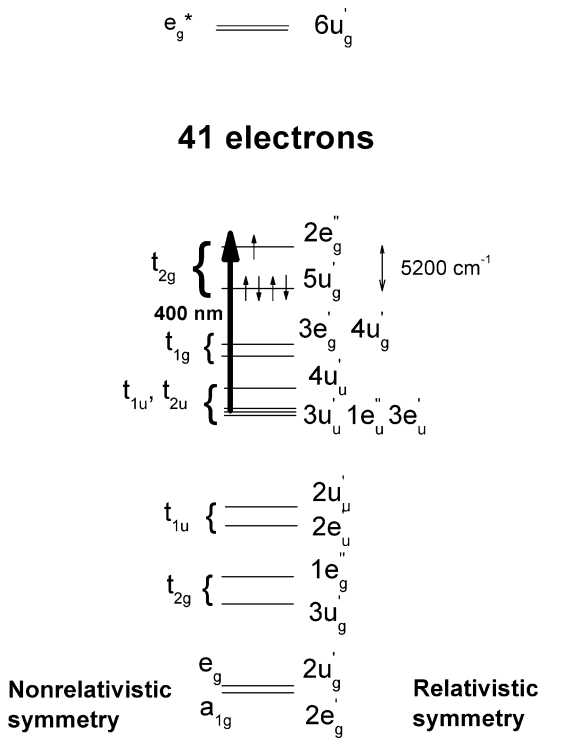

Fig. 2 The approximate structure of the molecular orbitals of the $IrCl_6^{2-}$ complex according to ref. 16 (non-relativistic approximation, left-hand side) and ref. 30 (relativistic approximation, right-hand side). Electrons in filled orbitals lower than $5u_g'$ are not shown. The bold arrow corresponds to 400 nm excitation.

However, the contribution of photoreduction to the quantum yield linearly increases with the concentration of chloride ions.

When $IrCl_6^{2-}$ is excited in the region of d–d bands (313 nm), the only photochemical reaction is photoaquation with a quantum yield of 0.01.[2] The mechanism of photolysis in this region was studied in ref. 4 using nanosecond laser flash photolysis (308 nm). Photolysis in the absence of free chloride ions was shown to result in photoaquation of initial complex within less than 20 ns. In solutions containing free Cl^- ions, the photoreduction of $IrCl_6^{2-}$ and the formation of the $Cl_2^{\bullet-}$ radical cation were observed. A chlorine atom, which is a precursor of the $Cl_2^{\bullet-}$ radical cation, is formed by an electron transfer from an outerspheric Cl^- ion to the light-excited complex.[4]

Excitation of $IrCl_6^{2-}$ in aqueous solutions in the region of visible charge-transfer bands (400–500 nm) does not result in any remarkable photochemical reactions.

Irradiation of $IrCl_6^{2-}$ in acetonitrile both in the region of UV charge transfer bands (254 nm) and d–d bands (313 nm) results in the stepwise solvation of the initial complex;[10] no redox processes are observed.

In simple alcohols, photoreduction of Ir(IV) to Ir(III) is followed by excitation both at 254 and 313 nm.[11,12] Excitation in the region of d–d bands results in the formation of the $IrCl_6^{3-}$ complex due to the electron transfer from the solvent molecule to the excited complex.[11,14] Irradiation of $IrCl_6^{2-}$ in methanol solutions in the region of the UV charge transfer bands (248 nm) results in the formation of two Ir(III) complexes, $IrCl_6^{3-}$ and $IrCl_5(CH_3OH)^{2-}$.[11] When photolysis is performed at 248 nm, the electron transfer from the solvent molecule is accompanied by photodissociation of the excited complex with the elimination of a chlorine atom from the first coordination sphere of iridium.[11] The part of the last channel is *ca.* 10%.[11]

The visible charge transfer bands of $IrCl_6^{2-}$ are not photoactive in alcohols, as in the case of aqueous solutions.

Primary photophysical processes are known in detail only for a few types of transition metal complexes (see *e.g.* ref. 18–22). For the case of the haloid complexes of noble metals the experiments with pico- and femtosecond time resolution are scarce.[23–26] In ref. 23, the $PtCl_6^{2-}$ complex was studied by means of picosecond laser flash photolysis. The authors of ref. 24 applied femtosecond photoelectron spectroscopy to examine the excited states dynamics of $IrBr_6^{2-}$ dianion in the gas phase. Primary photophysical processes were studied for aqueous solutions of $PtBr_6^{2-}$ [25,26] and $IrCl_6^{2-}$ [6] complexes.

In ref. 6, the photophysical processes for aqueous $IrCl_6^{2-}$ solutions were studied by means of ultrafast pump-probe spectroscopy with the excitation at 420 nm, *i.e.* in the region of the LMCT $^2T_{2u}$ state (the corresponding transition is marked by a bold arrow in Fig. 2). The visible charge transfer bands of $IrCl_6^{2-}$ are not photoactive. The excitation was followed by the formation of an intermediate absorption completely decaying with two characteristic times of 0.5 and 18 ps. Complete recovery of the ground state was consistent with the the absence of photochemical activity of the visible LMCT bands of $IrCl_6^{2-}$. Two possibilities of the lifetimes' interpretation were mentioned in ref. 6. The first possibility is that the fast process (τ_1 = 500 fs) is vibrational cooling of the hot $^2T_{2u}$* state, and the second process with the characteristic time τ_2 = 18 ps is the relaxation of the excited $^2T_{2u}$ state to the ground $^2T_{2g}$ state. Thermalization is probably accompanied by solvent relaxation. The second possibility is that the first characteristic time corresponds to the internal conversion of the Franck–Condon $^2T_{2u}$* state to the lowest excited state $^2T_{1g}$ accompanied by vibrational cooling, and the time τ_2 corresponds to the transition from the $^2T_{1g}$ to the ground state $^2T_{2g}$. Both interpretations do not seem to be contradictive. It is possible that both pathways can realize, and the two-exponential fitting curve represents a set of several exponential functions with close characteristic times.

In this work, the primary photophysical processes for $IrCl_6^{2-}$ complex in simple alcohols (methanol and ethanol) were examined by means of ultrafast pump-probe spectroscopy. An attractive task is to follow all the chain of phototransformations from the absorption of a light quantum to the final reaction products. The excitation was performed at 400 nm (LMCT $^2T_{2u}$ state, Fig. 2), which did not cause photochemical reactions. It allowed us to study the pure photophysics of the complex. The results were compared with the data for $IrCl_6^{2-}$ in aqueous solutions obtained in ref. 6.

2. Materials and methods

Solutions of $IrCl_6^{2-}$ complex were prepared from $Na_2IrCl_6 \cdot 6H_2O$ synthesized as described in ref. 27. The solutions were prepared using methanol and ethanol (Aldrich), which were used without additional purification. When necessary, the samples for stationary photolysis were deaerated by saturation with argon.

The UV absorption spectra were recorded using an Agilent 8453 spectrophotometer (Agilent Technologies). Laser photolysis (Fig. 1) was performed using the irradiation of an excimer laser (XeCl, 308 nm). The pattern of spectral changes for laser photolysis of $IrCl_6^{2-}$ was the same as for high pressure mercury lamp photolysis in the region of 313 nm.

An ultrafast pump-probe spectroscopy setup was described in detail elsewhere.[28] The samples were excited by ~60 fs pulses at ~400 nm (second harmonic of a Ti:sapphire generator–amplifier system, CDP Ltd., Moscow, Russia). The excitation pulse repetition rate was 10 Hz, and 200 pulses were used to record a single time-resolved spectrum. The samples were placed in a 1 mm rotating cell to provide a uniform irradiation of the sample and to avoid unwanted thermal effects from heating of the sample by the pump pulse. Typically time-resolved spectra were collected with delay displacement of 100 fs in the first 3 ps after excitation and with exponentially increasing delay times at longer delays. Usually 60–70 spectra were collected for each sample with the longest delay of ~100 ps. The experimental data were globally fitted by two- or three-exponential models. The fitting program performed corrections of the group velocity dispersion and calculated the response time of the instrument. The overall time resolution was 150–200 fs. All pump-probe measurements were carried out at room temperature.

3. Results and discussion

3.1. Photochemistry of $IrCl_6^{2-}$ in alcohol solutions

The mechanism of $IrCl_6^{2-}$ photolysis in alcohols, like in aqueous solutions, is wavelength-dependent, as it was mentioned in the Introduction. Excitation to the region of d–d bands (308 nm, Fig. 1) results in the photoreduction of the initial complex with the formation of the $IrCl_6^{3-}$ complex.[11,14] Fig. 1 shows the characteristic changes in the UV spectrum due to photoreduction. The occurring absorption band with the maximum at 209 nm belongs to $IrCl_6^{3-}$.[16,29] Disappearance of absorption in the visible spectral region is the result of an Ir(IV) → Ir(III) transition. The photolysis mechanism in deaerated methanol solutions is described by equations (1–3). The primary quantum yield of photoreduction determined by Reactions 1 and 2 is 0.1.[11] In deaerated solutions, Reaction 3 leads to the doubling of the quantum yield.[11] The formation of the final $IrCl_6^{3-}$ complex in Reactions 1 and 2 occurs on a time scale less than 20 ns.[11] In ethanol, the formation of the $CH_3^{\bullet}CHOH$ radical was observed.[14,15]

$$IrCl_6^{2-} \xrightleftharpoons{h\nu} (IrCl_6^{2-})^* \quad (1)$$

$$(IrCl_6^{2-})^* \xrightarrow{CH_3OH} IrCl_6^{3-} + {}^{\bullet}CH_2OH + H^+ \quad (2)$$

$$IrCl_6^{2-} + {}^{\bullet}CH_2OH \rightarrow IrCl_6^{3-} + CH_2O + H^+ \quad (3)$$

The excitation to the region of the visible LMCT bands (Fig. 2), as mentioned in the Introduction, does not result in any changes of the UV spectra of the initial complex.

3.2. Ultrafast pump-probe experiments

Femtosecond pump-probe experiments were performed with the excitation of $IrCl_6^{2-}$ to the region of the low-energy LMCT charge transfer band (400 nm, Fig. 1). The absorption of a light quantum by the complex leads to the formation of a transient absorption completely decaying in 100 ps. The kinetic curves at several wavelengths obtained in methanol solution are shown in Fig. 3. The global analysis of the time profiles in the wavelength range 450–750 nm by iterative reconvolution shows that the use of a three-exponential function (4) with the instrument response function fits well the experimental data. The optimal values of the characteristic times are $\tau_1 = 350$ fs, $\tau_2 = 2.2$ ps and $\tau_3 = 30$ ps.

$$\Delta D(\lambda,t) = A_1(\lambda)e^{-\frac{t}{\tau_1}} + A_2(\lambda)e^{-\frac{t}{\tau_2}} + A_3(\lambda)e^{-\frac{t}{\tau_3}} \quad (4)$$

Fig. 4 demonstrates differential intermediate absorption spectra corresponding to different times (*i.e.* the difference between the absorption of the sample after and before the laser pulse). These spectra are the results of the global fit of kinetic curves shown in Fig. 3. The total sum of amplitudes (curve 1) is the differential spectrum at zero time; the $A_2(\lambda) + A_3(\lambda)$ sum (curve 2) is the differential spectrum at the end of first process ($\tau_1 = 350$ fs). After disappearance of $A_2(\lambda)$ ($\tau_2 = 2.2$ ps), the $A_3(\lambda)$ amplitude is the last differential spectrum before the complete decay of transient absorption ($\tau_3 = 30$ ps). Immediately after excitation, the transient absorption spectrum has a wide band with the maximum in the region of 700 nm. After the end of the first process ($\tau_1 = 350$ fs) the pronounced maximum is shifted to 560 nm, and the band remains wide. After the end of the second process ($\tau_2 = 2.2$ ps) the maximum of the band is shifted to the region of 610 nm. No residual absorption is observed in the time domain >100 ps. The disappearance of the initial $IrCl_6^{2-}$ absorption in the region 440–500 nm (Fig. 4) is completely recovered (Fig. 3).

The processes observed after excitation (400 nm) of $IrCl_6^{2-}$ in ethanol solutions are similar to those characteristic for methanol

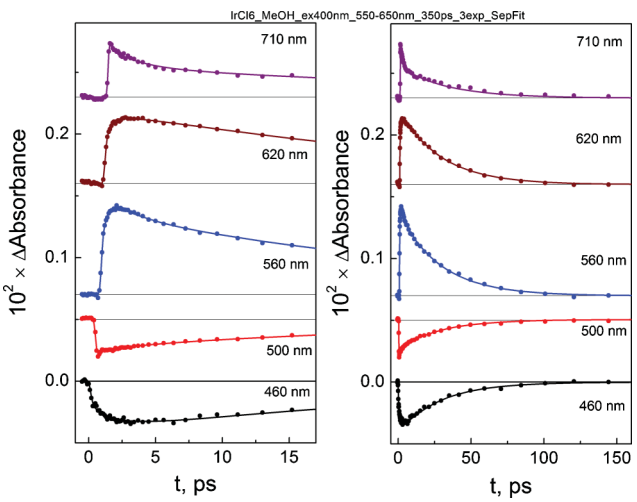

Fig. 3 Photolysis of $IrCl_6^{2-}$ (3×10^{-3} M) in methanol solution (λ_{pump} = 400 nm). Experimental kinetic curves of transient absorption at different wavelengths and time domains. Solid lines are the best three-exponential fits (eqn (4)) after reconvolution with the instrument response function. Wavelength-dependent time delay between $t = 0$ and the instantaneous rise part in the kinetics reflects the group velocity dispersion.

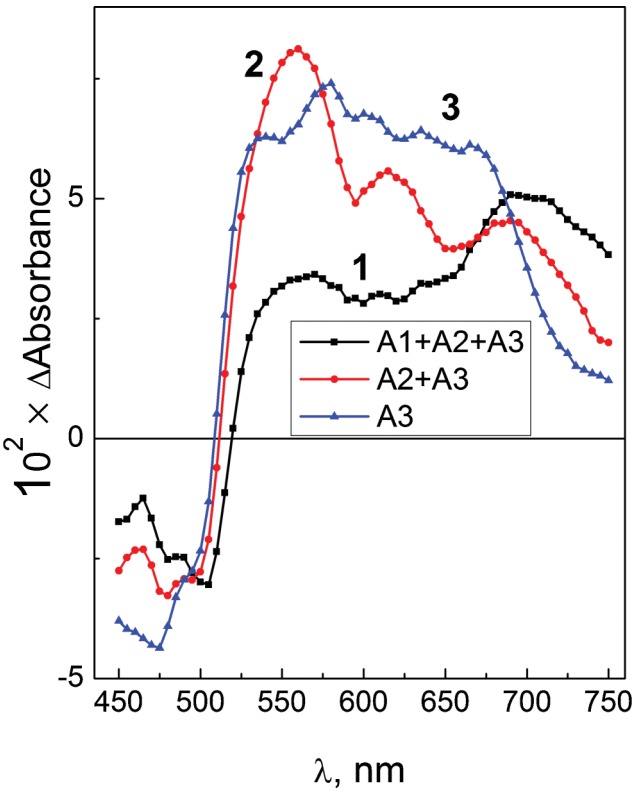

Fig. 4 Photolysis of $IrCl_6^{2-}$ (3×10^{-3} M) in methanol solution (λ_{pump} = 400 nm). Intermediate absorption spectra at different times. 3-exponential treatment of the data of Fig. 3. Curve 1 – zero time (sum of amplitudes $A_1(\lambda) + A_2(\lambda) + A_3(\lambda)$); curve 2 – after the end of the first process (sum of amplitudes $A_2(\lambda) + A_3(\lambda)$); curve 3 – after the end of the second process – (amplitude $A_3(\lambda)$, eqn (4)).

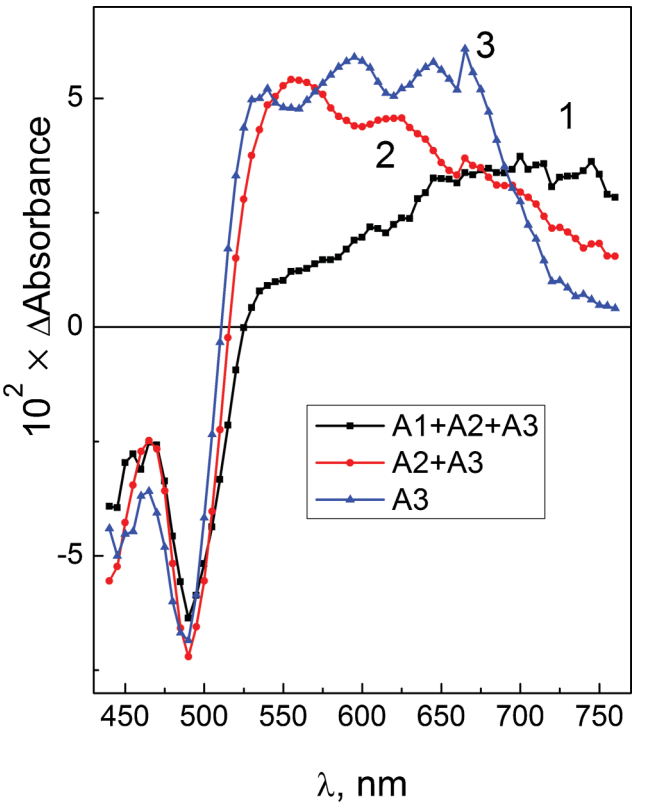

Fig. 5 Photolysis of $IrCl_6^{2-}$ (2.7×10^{-3} M) in ethanol solution (λ_{pump} = 400 nm). Intermediate absorption spectra at different times. 3-exponential treatment of kinetic curves. Curve 1 – zero time (sum of amplitudes $A_1(\lambda) + A_2(\lambda) + A_3(\lambda)$); curve 2 – after the end of the first process (sum of amplitudes $A_2(\lambda) + A_3(\lambda)$); curve 3 – after the end of the second process – (amplitude $A_3(\lambda)$, eqn (4)).

solutions. Again, the kinetic curves are well fitted by a three-exponential function (4) with the characteristic times close to that observed in methanol. Fig. 5 demonstrates intermediate absorption spectra in ethanol corresponding to different times. The information on the characteristic lifetimes is listed in Table 1. Table 1 also contains the data on the lifetimes of primary photophysical processes for $IrCl_6^{2-}$ in aqueous solutions obtained in ref. 6. In the last case, the minimal set of functions necessary for the fitting of the experimental data includes two exponential functions instead of three in the case of alcoholic solutions. Fig. 6 shows normalized spectra of $A_3(\lambda)$ amplitudes for alcohols and $A_2(\lambda)$ amplitude for aqueous solution. In fact, there are the spectra corresponding to the moments when all the fast processes (with the characteristic times < 3 ps) are over. These spectra are similar.

The absence of residual absorption both in alcoholic and aqueous solutions at $t > 100$ ps correlates with very low quantum yields of $IrCl_6^{2-}$ photolysis followed by excitation in the region of visible LMCT bands.[2]

3.3. Possible processes followed by the excitation of $IrCl_6^{2-}$ to the $^2T_{2u}$ LMCT band

In the framework of the simple non-relativistic description of $IrCl_6^{2-}$ spectroscopy, the excitation of $IrCl_6^{2-}$ in the region of 400–420 nm corresponds to the first Laporte-allowed LMCT band $\pi(t_{2u}) \rightarrow d(t_{2g})$.[17] As a result of an electron transfer, the hole moves from the lower 5d-sub-shell to the filled $\pi(t_{2u})$ molecular orbital of ligands, forming an only excited term $^2T_{2u}$.

Table 1 Characteristic lifetimes of intermediate absorption followed by excitation of the $IrCl_6^{2-}$ complex in the region of visible LMCT bands (400–420 nm). 3-exponential fit (eqn (4))

Solvent	τ_1	Process	τ_2	Process	τ_3	Process
	ps		ps		ps	
MeOH	0.35	$2U_u'^* \rightarrow 1U_g'^*$	2.2	$1U_g'^* \rightarrow 1U_g'$	30	$1U_g' \rightarrow 1E_g''$
EtOH	0.29		2.7		31	
H_2O^a	0.5	$2U_u'^* \rightarrow 1U_g'$	—		18	$1U_g' \rightarrow 1E_g''$

[a] Measured in ref. 6. In aqueous solutions the experimental kinetic curves were well fitted by a biexponential function.

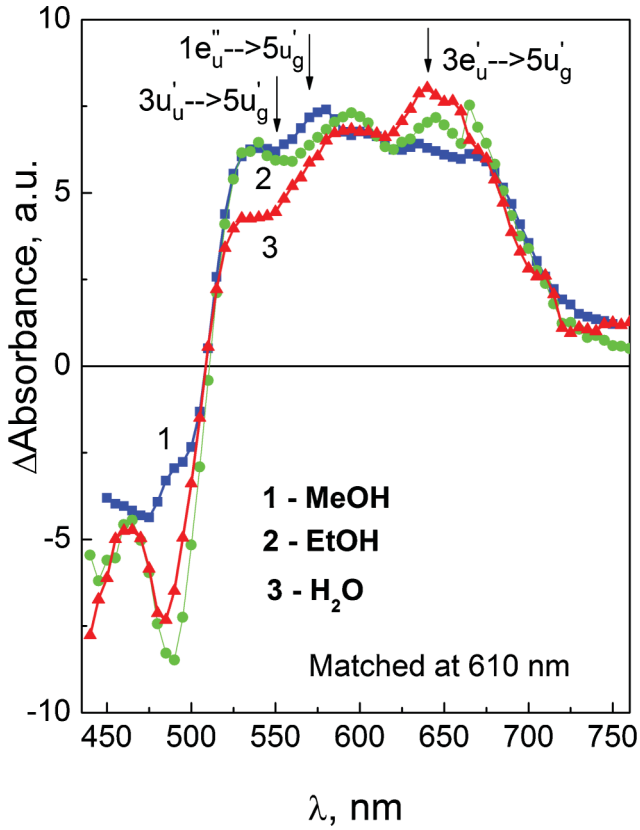

Fig. 6 $IrCl_6^{2-}$ photolysis in methanol (1), ethanol (2) and water (3). Intermediate absorption spectra after the end of ultrafast processes (amplitudes $A_3(\lambda)$, eqn (4)). For aqueous solutions $A_2(\lambda) \equiv 0$. Experimental curves are matched at 610 nm. Data for aqueous solutions were taken from ref. 6. Possible transitions to the $1U_g'$ state are indicated.

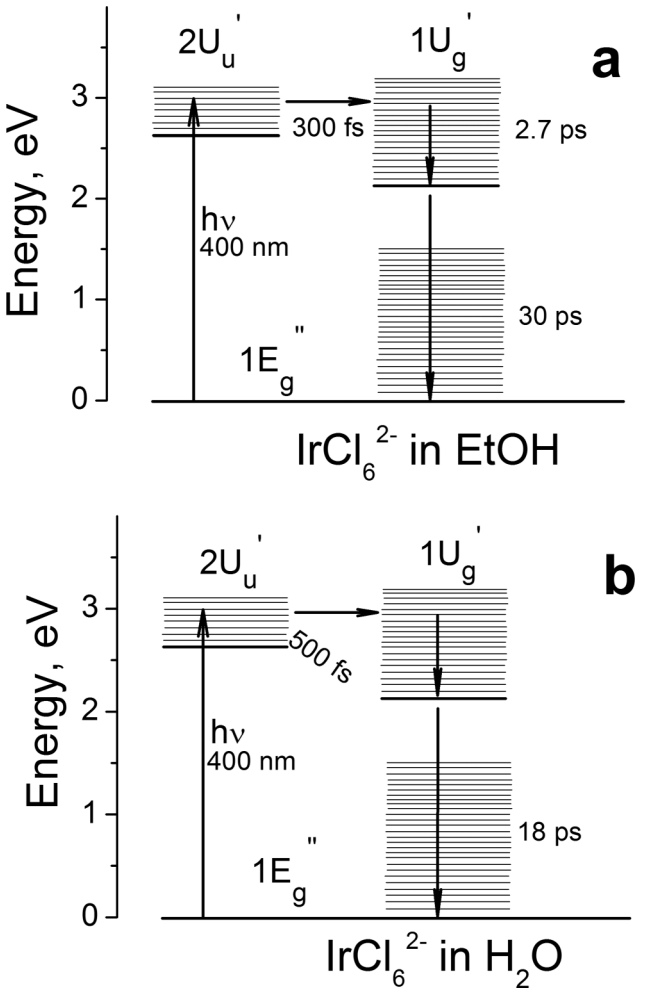

Fig. 7 A schematic representation of the processes followed by ultrafast excitation (400 nm) of $IrCl_6^{2-}$ in ethanol (**a**) and water (**b**).

The dramatic spectral changes occurring in *ca.* 300 fs (spectra 2 in Fig. 4 and 5) are indicative of the electronic transition. During the second process with the characteristic time 2–3 ps (spectra 3 in Fig. 4 and 5) the changes in the shape of the spectra are not large, which could be indicative of the vibrational (or solvent) relaxation. The similarity of the intermediate absorption at the time of several picoseconds in water, methanol and ethanol (Fig. 6) shows that the same electronic state is formed. The absence of further spectral changes indicates that this state is the lowest excited state $1U_g'$, which is formed by the electronic configuration with a hole in the $5u_g'$ orbital. This is a mixed metal–ligand state with *ca.* 50% of metal character lying *ca.* 5200 cm^{-1} lower than the ground state.[30] In the framework of this interpretation the spectra in Fig. 6 correspond to the transitions from the $1U_g'$ state. The wavelengths of the transitions corresponding to $3e_u' \rightarrow 5u_g'$, $1e_u'' \rightarrow 5u_g'$ and $3u_u' \rightarrow 5u_g'$ promotions (calculated using the results of ref. 30 and experimental spectrum in Fig. 1) are 641, 550 and 570 nm. It gives a quantitative description of the observed intermediate absorption spectra (Fig. 6).

In the framework of the proposed mechanism, the final characteristic time (18-31 ps in different solvents, Table 1) corresponds to the $5u_g' \rightarrow 2e_g''$ transition with an energy of *ca.* 23 kcal $mole^{-1}$. The proposed identification of all the observed processes for water and alcohols is given in Table 1 and Fig. 7.

The last point to discuss is why the kinetic curves in alcohols are fitted by a set of three exponential functions, while in aqueous solutions two exponents are sufficient.[6] The characteristic times of the formation of thermalized $1U_g'$ excited state are 500 fs in water and 2–3 ps in alcohols (Table 1). The relaxation of excited states includes several processes, which are vibrational relaxation, solvent relaxation (both nondiffusive and diffusive), and intersystem crossing.[18,19] In fact, the spectroscopic signatures of the vibrational relaxation dynamics and solvation dynamics are similar in pump-probe spectroscopy.[31] The different processes (*e.g.*, intersystem crossing and vibrational relaxation) could have similar characteristic times and manifest itself as a single, convoluted process.[18]

In the case of $IrCl_6^{2-}$ complex in aqueous solutions the first characteristic time (500 fs) includes both $3u_u' \rightarrow 5u_g'$ electronic transition and vibrational relaxation. In alcohol solutions, the first time (*ca.* 300 fs) corresponds to an electronic transition with the formation of the hot $1U_g'^*$ state. The second characteristic time (*ca.* 2.5 ps) could correspond to either vibrational relaxation or solvent diffusive relaxation. In addition, both these processes could be convoluted. Therefore, the relaxation processes in alcohols occur somewhat slower than in water.

It should be noted that the characteristic times of both solvation dynamics and relaxation dynamics dramatically depend on both solvent and solute nature.[32] The solvation dynamics are typically

biphasic with a very rapid (tens of femtoseconds) inertial solvation and much slower diffusional solvation.[32,33] The times of diffusional solvation in different solvents span more than three orders of magnitude, from ~0.1 ps to ~200 ps.[34,32] Water is the "fastest" solvent, which can stabilize polar reactants within 100 fs.[33] Direct measurements of *N*-methyl-6-quinone probe solvation [33] have demonstrated that the characteristic time of the longer component of solvation in methanol sufficiently exceeds that in water (*ca.* 10 and 1 ps).

The reported characteristic times of vibrational relaxation in water are also less than in organic solvents. The times of vibrational cooling of Ru(II)–Ru(III) metal dimers were measured to be 900 fs in water and 2.7 ps in formamide.[35] The vibrational population relaxation of SCN^- cation is 2.7 ps in water [36] and much slower in methanol (23 ps [37]) and other different organic solvents (25–70 ps[38]). Therefore, the results of current work do not contradict to the known experimental fact that the rate of solvent and vibrational relaxation in water is higher than in polar organic solvents.

Finally, the recovery of the initial state of $IrCl_6^{2-}$ (both in water and alcohols) is complete (Fig. 3), which corresponds to the absence of photochemical activity followed by the excitation of $IrCl_6^{2-}$ to the visible LMCT bands.

Conclusions

In this paper, the simplest case of LMCT excitation of $IrCl_6^{2-}$ was examined. Visible charge transfer bands of $IrCl_6^{2-}$ are not photoactive in both aqueous and alcohol solutions. Therefore, the experiments on femtosecond pump-probe spectroscopy with excitation at 400 nm allow one to examine the photophysical processes resulting in the recovery of the initial state. It was performed for $IrCl_6^{2-}$ in aqueous[6] and alcohol (this work) solutions. It seems very attractive to perform ultrafast experiments with the excitation in the region of d–d bands (*ca.* 300 nm) and UV charge transfer bands (<260 nm) in order to observe the initial states of photochemical reactions.

Acknowledgements

The work was supported by Russian Foundation of Basic Research (grants no. 11-03-00268, 09-03-00330) and Program of Integration Projects of SB RAS 2009-2011 (grant no. 70).

Notes and references

1 T. P. Sleight and C. R. Hare, *Inorg. Nucl. Chem. Lett.*, 1968, **4**, 165.
2 L. Moggi, G. Varani, M. F. Manfrin and V. Balzani, *Inorg. Chim. Acta*, 1970, **4**, 335.
3 P. K. Eidem, A. W. Mawerick and H. B. Gray, *Inorg. Chim. Acta*, 1981, **50**, 59.
4 E. M. Glebov, V. F. Plyusnin, N. V. Tkachenko and H. Lemmetyinen, *Chem. Phys.*, 2000, **257**, 79.
5 E. M. Glebov, V. F. Plyusnin, N. V. Tkachenko and H. Lemmetyinen, *Russ. Chem. Bull.*, 2008, **57**, 2487.
6 A. V. Litke, I. P. Pozdnyakov, E. M. Glebov, V. F. Plyusnin, N. V. Tkachenko and H. Lemmetyinen, *Chem. Phys. Lett.*, 2009, **477**, 304.
7 G. R. Gale, J. A. Howle and A. B. Smith, *Proc. Soc. Exp. Biol. Med.*, 1970, **135**, 690.
8 A. K. Gupta, R. Z. Parker and R. J. Hanrahan, *Int. J. Hydrogen Energy*, 1993, **18**, 713.
9 S. Fukuzumi and J. K. Kochi, *Inorg. Chem.*, 1980, **19**, 3022.
10 E. M. Glebov and V. F. Plyusnin, *Russ. J. Coord. Chem.*, 1998, **24**, 507.
11 E. M. Glebov, V. F. Plyusnin, N. I. Sorokin, V. P. Grivin, A. B. Venediktov and H. Lemmetyinen, *J. Photochem. Photobiol., A*, 1995, **90**, 31.
12 E. M. Glebov, V. F. Plyusnin, V. L. Vyazovkin and A. B. Venediktov, *J. Photochem. Photobiol., A*, 1997, **107**, 93.
13 E. M. Glebov, V. F. Plyusnin, V. P. Grivin, Yu. V. Ivanov, N. V. Tkachenko and H. Lemmetyinen, *J. Photochem. Photobiol., A*, 1998, **113**, 103.
14 E. M. Glebov, V. F. Plyusnin, V. P. Grivin, Yu. V. Ivanov, N. V. Tkachenko and H. Lemmetyinen, *Int. J. Chem. Kinet.*, 1998, **30**, 711.
15 E. M. Glebov, V. F. Plyusnin and V. L. Vyazovkin, *High Energy Chem.*, 1999, **33**, 390.
16 C. K. Jorgensen, *Mol. Phys.*, 1959, **2**, 309.
17 C. K. Jorgensen and W. Pretz, *Z. Naturforsch.*, 1967, **22a**, 945.
18 A. Vlcek Jr., *Coord. Chem. Rev.*, 2000, **200–202**, 933.
19 J. K. McCusker, *Acc. Chem. Res.*, 2003, **36**, 876.
20 L. S. Forster, *Coord. Chem. Rev.*, 2006, **250**, 2023.
21 N. Huse, K. K. Kim, L. Jamula, J. K. McCusker, F. M. F. de Groot and R. W. Schoenlein, *J. Am. Chem. Soc.*, 2010, **132**, 876.
22 J. N. Schrauben, K. L. Dillman, W. F. Beck and J. K. McCusker, *Chem. Sci.*, 2010, **1**, 405.
23 A. Goursot, A. D. Kirk, W. L. Waltz, G. B. Porter and D. K. Sharma, *Inorg. Chem.*, 1987, **26**, 14.
24 C. Rensing, O. T. Ehrler, J.-P. Yang, A.-N. Unterreiner and M. M. Kappes, *J. Chem. Phys.*, 2009, **130**, 234306.
25 I. P. Pozdnyakov, E.M. Glebov, V. F. Plyusnin, N. V. Tkachenko and H. Lemmetyinen, *Chem. Phys. Lett.*, 2007, **442**, 78.
26 I. L. Zheldakov, M. S. Panov and A. N. Tarnovsky, *Abstr. Pap. Am. Chem. Soc.*, 2008, **236**, 380-PHYS.
27 E. N. Sloth and C. S. Garner, *J. Am. Chem. Soc.*, 1955, **77**, 1440.
28 N. V. Tkachenko, L. Rantala, A. Y. Tauber, J. Helaja, P. H. Hynninen and H. Lemmetyinen, *J. Am. Chem. Soc.*, 1999, **121**, 9378.
29 I. A. Poulsen and C. S. Garner, *J. Am. Chem. Soc.*, 1962, **84**, 2032.
30 J. P. Lopez and D. A. Case, *J. Chem. Phys.*, 1984, **81**, 4554.
31 D. H. Son, P. Kambhampati, T. W. Kee and P. F. Barbara, *J. Phys. Chem. A*, 2002, **106**, 4591.
32 R. M. Stratt and M. Maroncelli, *J. Phys. Chem.*, 1996, **100**, 12981.
33 J. L. Perez Lustres, S. A. Kovalenko, M. Mosquera, T. Senyushkina, W. Flasche and N. P. Ernsting, *Angew. Chem., Int. Ed.*, 2005, **44**, 5635.
34 M. L. Horng, J. A. Gardecki, A. Papazyan and M. Maronchelli, *J. Phys. Chem.*, 1995, **99**, 17311.
35 P. J. Reid, C. Silva, P. F. Barbara, L. Karki and J. T. Hupp, *J. Phys. Chem.*, 1995, **99**, 2609.
36 Q. Zhong, A. P. Baronavski and J. C. Owrutsky, *J. Chem. Phys.*, 2003, **119**, 9171.
37 K. Dahl, G. M. Sando, D. M. Fox, T. E. Sutto and J. C. Owrutsky, *J. Chem. Phys.*, 2005, **123**, 084504.
38 K. Ohta and K. Tominaga, *Chem. Phys. Lett.*, 2006, **429**, 136.

